NeuroImage 200 (2019) 121–131

Contents lists available at ScienceDirect

NeuroImage

journal homepage: www.elsevier.com/locate/neuroimage

Association between the oral microbiome and brain resting state connectivity in smokers

Dongdong Lin [a,e,*], Kent E. Hutchison [b], Salvador Portillo [d], Victor Vegara [a,e], Jarrod M. Ellingson [b], Jingyu Liu [a,d,e], Kenneth S. Krauter [c], Amanda Carroll-Portillo [d,1], Vince D. Calhoun [a,d,e,1]

[a] The Mind Research Network, Albuquerque, NM, 87106, USA
[b] Department of Psychology and Neuroscience, University of Colorado Boulder, Boulder, 80309, USA
[c] Molecular,Cellular,and Developmental Biology, University of Colorado Boulder, Boulder, 80309, USA
[d] University of New Mexico, Department of Electrical and Computer Engineering, Albuquerque, NM, 87106, USA
[e] Tri-institutional Center for Translational Research in Neuroimaging and Data Science (TReNDS) [Georgia State University, Georgia Institute of Technology, Emory University], Atlanta, GA, 30303, USA

ARTICLE INFO

Keywords:
Microbiome
Neuroimaging
Functional connectivity
Saliva
Smoking

ABSTRACT

Recent studies have shown a critical role of the gastrointestinal microbiome in brain and behavior via the complex gut–microbiome–brain axis. However, the influence of the oral microbiome in neurological processes is much less studied, especially in response to the stimuli, such as smoking, within the oral microenvironment. Additionally, given the complex structural and functional networks in brain, our knowledge about the relationship between microbiome and brain function through specific brain circuits is still very limited. In this pilot study, we leveraged next generation sequencing for microbiome and functional neuroimaging technique to enable the delineation of microbiome-brain network links as well as their relationship to cigarette smoking. Thirty smokers and 30 age- and sex-matched nonsmokers were recruited for 16S sequencing of their oral microbial community. Among them, 56 subjects were scanned by resting-state functional magnetic resonance imaging to derive brain functional networks. Statistical analyses were performed to demonstrate the influence of smoking on the oral microbial composition, functional network connectivity, and the associations between microbial shifts and functional network connectivity alternations. Compared to nonsmokers, we found a significant decrease of beta diversity ($P = 6 \times 10^{-3}$) in smokers and identified several classes (Betaproteobacteria, Spirochaetia, Synergistia, and Mollicutes) with significant alterations in microbial abundance. Pathway analysis on the predicted KEGG pathways shows that the microbiota with altered abundance are mainly involved in pathways related to cell processes, DNA repair, immune system, and neurotransmitters signaling. One brain functional network connectivity component was identified to have a significant difference between smokers and nonsmokers ($P = 0.032$), mainly including connectivity between brain default network and other task-positive networks. This brain functional component was also significantly associated with smoking related microbiota, suggesting a correlated cross-individual pattern between smoking-induced oral microbiome dysbiosis and brain functional connectivity alternation, possibly involving immunological and neurotransmitter signaling pathways. This work is the first attempt to link oral microbiome and brain functional networks, and provides support for future work in characterizing the role of oral microbiome in mediating smoking effects on brain activity.

1. Introduction

Nicotine, an addictive substance, has been reported to influence brain function and human behavior, including cognitive function and endogenous information processing networks (Fedota and Stein, 2015). Functional magnetic resonance imaging (fMRI) has been widely applied to delineate the interactions among diverse brain functional networks related to nicotine use or dependence, informing our understanding of

* Corresponding author. The Mind Research Network, Albuquerque, NM, 87106, USA.
E-mail address: dlin@mrn.org (D. Lin).
[1] Authors contributed equally to the work.

https://doi.org/10.1016/j.neuroimage.2019.06.023
Received 13 December 2018; Received in revised form 11 June 2019; Accepted 11 June 2019
Available online 13 June 2019

the links between brain function and smoking abuse or cessation. Studies have reported negative association between the severity of nicotine dependence and dorsal anterior cingulate cortex (dACC) connectivity strength with several other regions including the striatum and insula (Hong et al., 2009; Moran et al., 2012). These studies suggest the use of resting state connectivity among dACC, insula and striatum as biological measures of nicotine addiction. Consistent reduction of dACC-insula connectivity was also found in smokers who relapsed when quitting compared to those who remained abstinent (Janes et al., 2010). Cole et al. (2010) reported that cognitive withdrawal improvement after nicotine replacement was associated with enhanced connectivity between the executive cognitive network (ECN) and the default mode network (DMN). After acute nicotine administration, nonsmokers showed reduced activity within the DMN and increased activity in extra-striate regions within the visual attention network, suggesting a shift in network activity from internal to external information processing (Tanabe et al., 2011). Other evidence supports the critical role of insula, together with the ACC in influencing the dynamics between large-scale brain networks (Fedota and Stein, 2015). Significant lower connectivity strength between left ECN and DMN domains was found in chronic smokers compared to nonsmokers (Weiland et al., 2015). Chronic nicotine use also showed negative impact on functional network connectivity within ECN domain.

Smoking can affect oral health by altering the microbial ecosystem in the oral cavity. There are around 600 types of bacterial species inhabiting the human oral cavity, which live together in synergy (Dewhirst et al., 2010). Bacteria can colonize and form complex communities in the oral cavity on a range of surfaces including on the teeth, the tongue, or under the gum with each surface representing a specific microenvironment with slightly variant conditions. The oral microbiome helps to maintain oral health, but composition is sensitive to environmental disruptions including smoking cigarettes or antibiotic intake (Wade, 2013). The balance of the microbial ecosystem is disturbed by these alterations, namely dysbiosis, which can result in diseases such as periodontitis or respiratory diseases (Camelo-Castillo et al., 2015; Morris et al., 2013; Warinner et al., 2014). Smoking can directly influence the oral microbiome and perturb oral microbial ecology through a variety of mechanisms including antibiotic effects or oxygen deprivation (Macgregor, 1989). Evidence suggests that smoking can drive colonization of marginal and subgingival spaces with highly diverse biofilms to result in a pro-inflammatory response from the host (Kumar et al., 2011). Investigators also found that smokers harbored more pathogenic, anaerobic microbes in the subgingival space than nonsmokers (Mason et al., 2015). Study by 16S RNA sequencing has demonstrated a shift in the abundances of particular microbiota in smokers compared to nonsmokers, including an increase in pathogenic microbes associated with increased risk of oral diseases (Shchipkova et al., 2010). Kumar et al. identified an increase in periodontal pathogens belonging to the genera *Fusobacterium*, *Cardiobacterium*, *Synergistes*, and *Selenomonas* in tobacco users (Kumar et al., 2011). Wu et al. showed depletion in the abundance of oral health related microbiota including the phylum Proteobacteria and genera *Capnocytophaga*, *Peptostreptococcus* and *Leptotrichia* in smokers, which could potentially lead to smoking-related diseases (Wu et al., 2016).

In the past few years, many studies have shown a critical role of the gastrointestinal microbiome in brain development, function, and behavior via the complex gut microbiome–brain axis (Borre et al., 2014; Collins et al., 2012). It has been suggested that the communications between the microbiome and brain is bidirectional through multiple pathways including the hypothalamic-pituitary-adrenal axis (HPA), neurotransmitter pathways, immune system, and recognition of bacterial or host metabolites. Research has found that hormonal changes along the HPA axis due to neurological reactions within the brain to stress or anxiety are related to gut microbiome composition (Sudo et al., 2004). Inversely, gastrointestinal microbial perturbations have been shown to impair recognition memory and cognitive function in hippocampus (Gareau et al., 2011). Microbiota are also involved in several neurotransmitter pathways including dopaminergic, serotonergic, and glutamatergic signaling, which are well known in modulating neurogenesis and brain function (O'mahony et al., 2015). Animal models have also demonstrated increased levels of noradrenaline, dopamine, and serotonin in the striatum and hippocampus, and reduced expression of N-methyl-D-aspartate receptor subunits in the hippocampus, cortex, and amygdala in germ-free mice, suggesting the role of the microbiome in regulating the levels of these neurotransmitters in the brain (Foster and Neufeld, 2013). The microbiome has also been reported to affect neurogenesis and development given its possible influence on brain-derived neurotropic factor expression in multiple brain regions. Moreover, neuroinflammation also plays a critical role in brain and behavioral abnormalities, disrupting synaptic plasticity and neurogenesis among cortical and limbic areas (Spear, 2018). Certain bacteria (e.g., Bacteroidetes) are believed to stimulate neuroinflammation via increased brain-blood-barrier permeability and toll-like receptor 4 (TLR4)-mediated inflammatory pathways (Round et al., 2011). With such a close relationship between the gastrointestinal microbiome and brain function, researchers have identified several neurological disorders correlated to changes in gastrointestinal microbial populations including autism, major depression disorders, and neurodegenerative disorders (Mulle et al., 2013; Jiang et al., 2015; Quigley, 2017).

While most studies focus on the influence of gut microbiome on brain signaling, the potential role of the oral microbiome in the regulation of neurological activity is much less studied. Recent work has demonstrated that oral microbial perturbations are associated with neurodegeneration (e.g., Alzheimer's diseases, Parkinson's disease, and glaucoma) (Shoemark and Allen, 2015; Astafurov et al., 2014; Pereira et al., 2017). Bacterial endotoxin from the oral cavity is tied to chronic, subclinical inflammation, development of neurodegeneration, and has even been related to the patients suffering from Alzheimer's disease (Shoemark and Allen, 2015). As the second most taxonomically diverse body site, the oral microbiome consists of some bacteria that are specific to the oral cavity while also sharing microbes found within the in gastrointestinal microbiome. As such, it is not surprising that some oral and gut microbiota show concordant disease associations (Said et al., 2014) indicating a potential connection between the two sites contributing to inflammatory diseases (Cao, 2017; Chen et al., 2010). With these linkages and close proximity to the brain, there is high potential for oral dysbiosis, similar to gastrointestinal dysbiosis, to affect brain activity. However, knowledge of the constituents and interactions of the oral microbiome is still limited, especially in relation to how the compositional changes influence neurological signaling in the context of disease.

Despite recent advances in understanding of the gut-brain axis, there is still a significant gap in knowledge as to the role of the microbiome on different regions or circuits involved in brain function. However, neuroimaging can enable the delineation of microbiome influences on brain circuitry for specific conditions, e.g., substance use. Recent studies have identified the influence of changes in the gastrointestinal microbiome to activation of brain circuits related to memory and depression (Bagga et al., 2018; Tillisch et al., 2013; Pinto-Sanchez et al., 2017), suggesting the potential of combining the microbiome and neuroimaging in studying microbiome-brain interactions. However, there have not been investigations into the link between the oral microbiome and brain function in relation to behavioral changes. Smoking directly influences the constitution of the oral microbiome, which allows for examination of fluctuations in brain activities that are potentially correlated with shifts of the oral microbial composition. In this work, we leveraged next generation 16s rRNA sequencing and resting-state fMRI (rsfMRI) techniques to explore the effects of oral microbiome changes on brain function in relation to smoking. Saliva samples and resting-state fMRI scans from 60 individuals(i.e., smokers and nonsmokers) were collected, and the associations between bacterial populations and neurological signaling (e.g., brain functional connectivity) were examined. to demonstrate the relationshp among oral microbiome , brain function and smoking.

2. Materials and method

2.1. Participants

Sixty subjects were used for the analyses, including 30 smokers with the nicotine dependence score (FTQ: Fagerstrom Tolerance Questionnaire (Heatherton et al., 1991)) >6 and 30 age- and sex-matched, nonsmokers (FTQ score ≤6). Subjects consisted of 45 males and 15 females (Fisher exact test $p = 1$) between the ages of 21 and 56 (37.2 ± 10.65; $p = 0.98$). Group difference tests on age, AUDIT score (the alcohol use disorders identification test (Babor et al., 2001)), and marijuana smoking (the number of marijuana smoking days) via two-sample *t*-test, and sex by Chi-square test can be seen in Table 1. Among them, 56 subjects were matched with both microbiome and rsfMRI data, as listed in Table S1. Individuals have not previously been treated for nicotine use (e.g., varenicline) and had no serious medical or psychiatric conditions diagnosed within the past 6 months. Subjects with brain injury, brain-related medical problems, bipolar or psychotic disorders, illicit drugs use (confirmed through urinalysis), or currently taking insulin or oral hypoglycemic medication were excluded. In addition, to validate pathway analysis results, oral microbiome sequencing from additional 68 subjects were included.

Fig. 1 shows the overflow for integrative analysis of brain functional connectivity from rsfMRI and oral microbiome by 16*S* sequencing in smoking and nonsmoking groups. RsfMRI data are preprocessed by group independent component analysis (GICA) method (Calhoun et al., 2001) to derive independent functional networks and calculate functional network connectivity (FNC) matrix. FNC matrix is further decomposed by ICA into the multiplication by FNC loadings and FNC components for subsequent analysis. Microbiome sequencing data are preprocessed to generate a taxonomic table at different levels, characterize the diversity of the microbial community, and predict functional pathways. The features (e.g., FNC loading and taxonomic count) from both datasets are tested for associations with smoking status and FTQ score as well as their associations at difference scales (e.g., taxonomy, pathway).

2.2. 16S rRNA sequencing

Saliva samples were collected for 16S rRNA amplicon sequencing. Participants provided 5 mL of saliva in a sterile 50 mL conical centrifuge tube and stored in a refrigerator until the DNA was extracted. Sequencing was performed using an Illumina MiSeq covering variable region V4 with primers (5′GGAGGCAGCAGTRRGGAAT-3′ and 5′-CTACCRGGGTATTAAT -3′). Raw sequence data were demultiplexed and quality controlled by applying the pipeline in DADA2 (Callahan et al., 2016) to generate unique sequences. These unique sequences were similar to operational taxonomic units (OTU) in the previous pipeline with 100% clustering accuracy (Rideout et al., 2014). Each sequence was trimmed by the base quality (minimum Phred score = 30) and was aligned by the MAFFT tool to build a phylogenetic tree (Katoh and Standley, 2013). A classifier for taxonomy assignment was trained based on sequences and taxonomic results from the Greengenes database (http://greengenes.lbl.gov) with a 99% similarity. The classifier was then applied to the identified sequences (i.e., OTUs) for taxonomic assignment. Assigned sequences were further agglomerated to obtain taxonomic information at different levels (e.g., species, genus and class) for analyses. All processing scripts were implemented on a QIIME2 (https://qiime2.org/) platform.

Table 1
Demographics of subjects.

	Smoker (n = 30)	Nonsmoker (n = 30)	p
Age	37.23 ± 9.58	37.17 ± 11.78	0.98
Sex(M/F)	21/8	20/7	1
Alcohol (AUDIT score)	8.43 ± 9.27	14.1 ± 7.55	0.012
Marijuana smoking	12.27 ± 25	5.57 ± 13.11	0.2
FTQ score	8.87 ± 1.57	0.93 ± 1.96	—

2.3. Analysis of oral microbiome

We tested the overall difference in microbiota composition between smoking and non-smoking groups by comparing cross-sample distance measures. Raw read counts were first rarefied at 2020 sequences/sample. Weighted and unweighted UniFrac distance and Bray-Curtis distance were assessed by the R package 'vegan' (Oksanen et al., 2007) and tested for group difference by applying permutational MANCOVA ('Adonis' function in vegan package) controlling for age, sex, alcohol AUDIT score, and marijuana smoking score. Principal coordinate analysis (PCoA) plots were generated based on the first two principle coordinate vectors (i.e., eigenvectors) from each type of distance matrix to demonstrate the dissimilarity among samples in the 2-D space.

The taxonomic table was normalized to the relative abundances at different taxa levels. Taxa presented in less than 20% of subjects were filtered out, resulting in 163 OTUs, 73 genera, and 20 classes. Each taxon was tested for relative abundance difference between smoking and non-smoking groups by Wilcox ranked sum test. Those taxa with significant group difference, were further tested controlling for age, sex, alcohol and marijuana smoking by '*Zig*' function (zero-inflated gaussian mixture model) in the *MetagenomeSeq* package (Paulson et al., 2013). The '*Zig*' method has demonstrated the advantage in microbiome data analysis by modeling raw counts using multivariate Gaussian distribution and taking into account zero abundance in a large proportion of subjects for each taxon.

2.4. Resting state fMRI imaging

Fifty-six participants had resting state functional MRI (rsfMRI) collected on a 3 T S TIM Trio (Erlangen, Germany) scanner. Images were acquired with an echo-planar imaging (EPI) sequence (TR = 2000 ms, TE = 29 ms, flip angle = 75°) with a 12-channel head coil. Each volume consisted of 33 axial slices (64×64 matrix, 3.75×3.75 mm^2, 3.5 mm thickness, 1 mm gap). Image preprocessing was performed as previously described (Vergara et al., 2017). Briefly, this included slice-timing correction, realignment, co-registration and spatial normalization. By transforming the images to the Montreal Neurological Institute (MNI) standard space, we filtered out those with the root mean square of head movement exceeding 3 standard deviations, despiked time courses (Power et al., 2012), and smoothed images using a FWHM Gaussian kernel of size 6 mm. The data were then analyzed by group independent component analysis (GICA) (Calhoun et al., 2001) with 120 and 100 components for the first and second decomposition levels respectively (Calhoun et al., 2001; Erhardt et al., 2011). Thirty-nine out of the 100 components were selected with low noise and free of major artifacts. The spatial map of each selected component was z-transformed, and voxel-wise one-sample *t*-test statistics were thresholded to identify the brain areas as a functional network. The time course corresponding to each functional network was filtered using a band-pass filter 0.01–0.15 Hz. Finally, resting state FNC matrix was calculated for each subject based on the correlation coefficients between the time courses of all possible pairs formed with the 39 chosen functional networks.

2.5. Analysis of resting state fMRI imaging

Each element in the FNC matrix indicates the correlation between any two functional networks within the brain. We transformed the FNC matrix of each subject to the vector and concatenated all FNC matrices across all subjects to form the matrix $\boldsymbol{C}$ with a dimension of n (subjects) by m (FNCs). To reduce the dimension of large number of FNCs and improve the detection by accounting for the covariance structure among FNCs, we applied the ICA algorithm to decompose matrix $\boldsymbol{C}$ into the multiplication of two full rank matrices by $\boldsymbol{C} = \boldsymbol{AS}$, where matrix $\boldsymbol{S}$ contains independent FNC components and each represents a specific

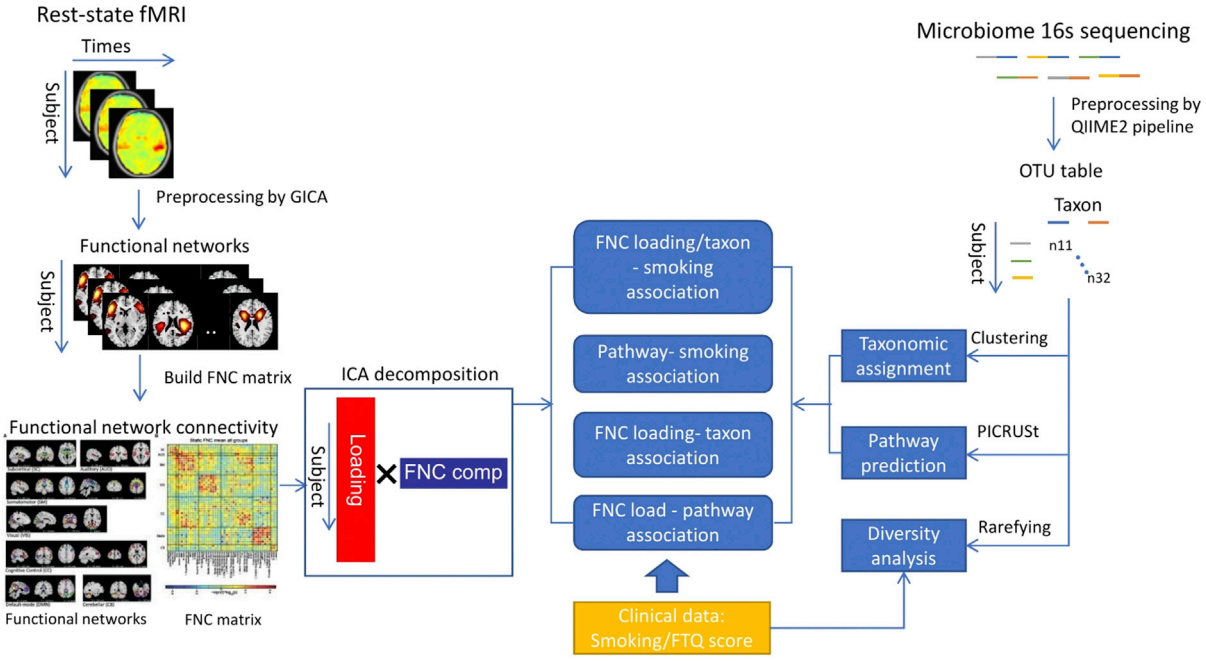

Fig. 1. The analysis overflow for resting state fMRI and oral microbiome 16S sequencing data in smokers and nonsmokers.

'source' mainly consisting of a cluster of FNCs with covariance structure. Matrix ***A*** contains the FNC loadings and each corresponds to a FNC component. FNC loading, different from FNC, shows the pattern of a cluster of FNCs across individuals, indicating the individual presentation of FNC component. The ICASSO algorithm (Ma et al., 2011) followed by best run selection was applied to obtain four reliable FNC components and each corresponding loading was tested for group difference by two-sample *t*-test. For the component with significant group difference, multiple regression model was further applied by controlling for covariates.

2.6. Linking microbiota with FNC

After obtaining significant FNC component and taxa from the above analyses, we further tested the association between the FNC loading and taxa using the '*Zig*' function with the following model design:

$$\text{Taxon} \sim \text{FNC loading} + \text{smoking status} + \text{age} + \text{sex} + \text{alcohol} + \text{marijuana}$$

The associations were tested at species, genus, and class levels. For each pair of associated taxon and FNC loading, top contributing FNCs from the FNC component will be tested for association with each taxon to delineate the relationship between FNC and taxa.

To further evaluate the influence of smoking in the microbiome-FNC component association, we added the interaction term (FNC loading × smoking status) in the above model. The significance for the interaction coefficient indicates if the association is different between smokers and nonsmokers. All tests were corrected for multiple testing by false discovery rate (FDR, Benjamin-Hochberg method).

2.7. Functional analysis of predicted metagenomes

Metagenome content in the samples was inferred from 16S rRNA microbial data, normalized by copy number count to account for the differences of the number of 16S rRNA copies between taxa, and then functional metabolic pathways were predicted based on the Kyoto Encyclopedia of Gene and Genomes (KEGG) catalog (Kanehisa and Goto, 2000), using Phylogenetic Investigation of Communities by Reconstruction of Unobserved States (PICRUSt) (Langille et al., 2013). Analyses revealed prediction of 328 metabolism pathways at level 3. Of these, 66 pathways were removed due to low sample occurrence (e.g., present in less than 10% of samples). Group difference of each metabolism pathway between smokers and nonsmokers was tested using Welch's *t*-test using the Statistical Analysis of Metagenomic Profiles (STAMP) software (Parks et al., 2014). Multiple comparisons were corrected by FDR with cut-off set as 0.15 for significance given the limited sample size in each group. The same pathway analysis was also performed in a larger sample size (including 68 additional individuals with oral microbiome sequencing) for validation. For the KEGG pathways and taxa significantly associated with smoking status, we further used Spearman's rank correlation to examine their relationship. The association between the identified KEGG pathways and FNC loading was also evaluated controlling for covariates.

3. Results

3.1. Overall microbiome composition between smoking groups

To determine whether overall oral microbiome composition differed between smokers and nonsmokers, we performed principal coordinate analysis on unweighted UniFrac, weighted UniFrac and Bray-Curtis phylogenetic distances. As shown in Fig. 2, without controlling for covariates, we found significant group difference in unweighted UniFrac distance ($p = 6 \times 10^{-3}$) and Bray-Curtis distance ($p = 0.025$) under 9999 times permutation. The differences were still significant ($p = 4 \times 10^{-3}$ and 0.027, respectively) after controlling for covariates (age, sex, alcohol score and marijuana smoking). No significant differences were found in weighted UniFrac ($p = 0.2$).

3.2. Taxonomic analysis between smokers and nonsmokers

To determine the compositional differences of microbiome between smokers and nonsmokers, we examined the relative abundance of taxa at the species, genus, and class levels. For each taxon, we tested their group difference using non-parametric rank sum test. For taxon with significant group difference (FDR$\leq$ 0.05), a multivariate test was applied controlling for covariates (age, sex, alcohol score and marijuana smoking). Fig. S1 and Table 2 show the relative abundance and log fold change (logFC = log2(smokers/nonsmokers)) of significant taxa by multivariate

test at the species, genus, and class levels. We found that class *Betaproteobacteria* significantly differed in smokers with a clear depletion as compared to nonsmokers (logFC = −0.35, FDR = 3.9×10^{-2}). Within this class, it was genera *Lautropia* (logFC = −1.99, FDR = 9.7×10^{-3}) and *Neisseria* (logFC = −1.16, FDR = 9.7×10^{-3}) that were specifically reduced in smokers. Other genera displaying significant differences between smokers and nonsmokers included *Treponema* (class Spirochaetes), *TG5* (class Synergistia), and *Mycoplasma* (class Mollicutes), which all had significant enrichment in smokers. Additionally, within the smoking population, there was a significant increase in relative abundance of genus *Bacteroides* (logFC = 2.24, FDR = 2.1×10^{-3}) that was not seen at the class level.

Lower-level analyses on OTUs identified 12 species from 7 classes showing significant difference between smoking and non-smoking groups. Besides the classes identified at the genus level, we additionally found 2 species from genus *Actinomyces* and *Rothia* in class Actinobacteria with higher abundance in smokers compared to nonsmokers. The abundance of three species from genera *Tannerella* and *Prevotella* (in class Bacteroidia) and one from genus *Fusobacterium* were also significantly increased in smokers. On the contrary, 2 species from genera *Oribacterium* and *Selenomonas* were depleted in smokers.

For these identified smoking-related taxa, we tested their associations with smoking FTQ score. As shown in Table S2, we found that most taxa had consistently significant associations with FTQ score as shown in Table 2 except genera *Neisseria* (FDR = 0.11) and *Lautropia* (FDR = 0.12) from class *Betaproteobacteria.*

3.3. Differential FNC component between groups

Among four rsfMRI components derived by applying ICA on the FNC matrix, there was one component with the corresponding loading vector showing marginal difference between smoking and non-smoking groups (P = 0.032, uncorrected), as shown in Fig. 3A. The group difference remained significant after controlling for covariates (P = 0.04, uncorrected) suggesting higher loading in smokers compared to nonsmokers for the FNC component. All of the top 13 FNCs with absolute (z-scored weights) > 2.5 in the component had negative weights (Fig. 3B), which indicates that those FNCs contributed in an opposite way to the component and therefore demonstrated significant reduction in smoking group. Fig. 3C shows the connectivity among functional networks from the top contributing FNCs in the component. The brain regions of those connected functional networks were plotted in Fig. 3D. Altered connectivity was mainly between DMN and visual network (VIS), salience network (SAL), and cognitive controls network (ECN), as well as between precunes (PRE) network and VIS. As listed in Table S3, the DMN network included several functional regions including anterior cingulate cortex (ACC), left angular gyrus and posterior cingulate cortex (PCC) with some precuneus overlap. The VIS group was composed of right fusiform/lingual gyrus, left middle occipital gyrus and right inferior occipital gyrus. The FNCs between DMN and other task-positive networks (VIS domain, inferior frontal gyrus (IFG) within the ECN domain, right supramarginal gyrus within the SAL domain, precuneus from PRE domain and supplementary motor area from SEN domain) were all negative, indicating stronger anti-correlation between DMN and those task-positive networks in smokers.

3.4. Association test between FNC component and microbiome

After identifying both taxa and FNC component showing significant group difference, we further tested for associations between the abundance of each taxon and the corresponding FNC loading as well as the interaction between FNC loading and smoking. Table 3 lists significant associations between taxa and FNC loading. The abundance of *Treponema* (class *Spirochaetes*), and *TG5* (class *Synergistia*) were positively associated with the FNC loading of the component while *Neisseria* (class *Betaproteobacteria*) demonstrated an opposite relationship. There were also significant interactions between FNC loading and smoking (P_interact = 0.044, 0.065 and 4.8×10^{-3}, respectively) in these microbiome-brain connectivity associations, suggesting association differences between the smoking and non-smoking groups. Further pair-

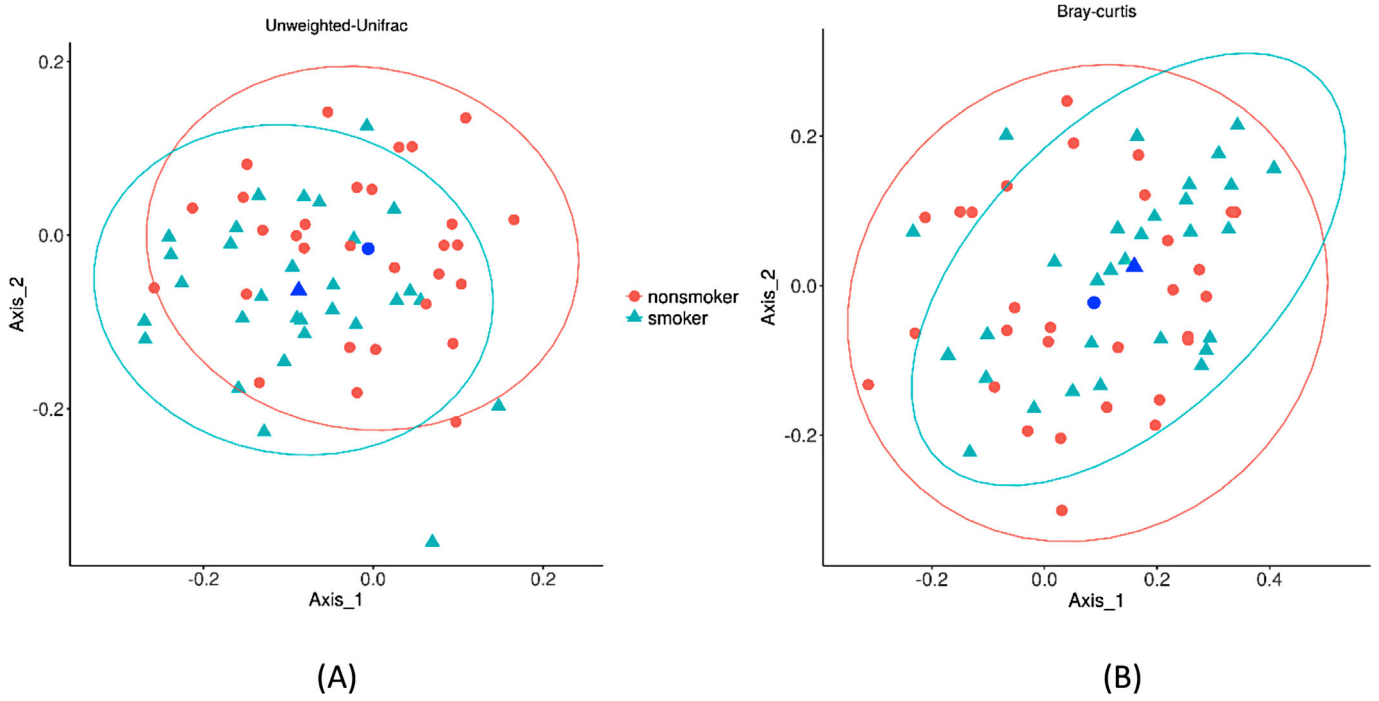

Fig. 2. PCoA analysis of microbial composition between smokers and nonsmokers. The microbial composition was evaluated based on (A) Unweighted UniFrac distance and (B) Bray-Curtis distance, respectively. Dark blue circle and triangle point indicates the center of eclipse for nonsmokers and smokers, respectively. Axis_1 and Axis_2 are the top two principle coordinate vectors (i.e., eigenvectors) from each distance matrix to visualize the distances among subjects in 2-D space.

Table 2
List of taxa with significant difference in relative abundance between smoking and non-smoking groups at species, genus and class levels.

Taxa					Relative Abundance			
Class	Order	Family	Genus	Species	Smoker	Nonsmokers	logFC	FDR
Species level								
Actinobacteria	Actinomycetales	Actinomycetaceae	Actinomyces	spp	7.8×10^{-3}	1.5×10^{-3}	2.35	1.2×10^{-3}
Actinobacteria	Actinomycetales	Micrococcaceae	Rothia	mucilaginosa	1.6×10^{-2}	6.3×10^{-3}	1.39	3.2×10^{-3}
Bacteroidia	Bacteroidales	Porphyromonadaceae	Tannerella	forsythia	1.1×10^{-3}	4.1×10^{-4}	1.42	2.4×10^{-2}
Bacteroidia	Bacteroidales	Prevotellaceae	Prevotella	oris	1.7×10^{-3}	7.1×10^{-4}	1.23	7.4×10^{-3}
Bacteroidia	Bacteroidales	Prevotellaceae	Prevotella	spp	7.1×10^{-4}	2.8×10^{-4}	1.32	2.4×10^{-2}
Clostridia	Clostridiales	Eubacteriaceae	Eubacterium	saphenum	7.9×10^{-4}	1.0×10^{-4}	2.92	1.5×10^{-3}
Clostridia	Clostridiales	Lachnospiraceae	Oribacterium	asaccharolyticum	1.4×10^{-3}	2.9×10^{-3}	−1.04	3×10^{-2}
Clostridia	Clostridiales	Veillonellaceae	Selenomonas	spp	1.9×10^{-3}	5.5×10^{-3}	−1.52	5×10^{-3}
Fusobacteria	Fusobacteriales	Fusobacteriaceae	Fusobacterium	nucleatum	9.8×10^{-3}	4.5×10^{-3}	1.14	8×10^{-2}
Betaproteobacteria	Burkholderiales	Burkholderiaceae	Lautropia	mirabilis	9.9×10^{-4}	4.1×10^{-3}	−2.06	7×10^{-3}
Synergistia	Synergistales	Dethiosulfovibrionaceae	TG5	unclassified	7.7×10^{-4}	1.4×10^{-4}	2.44	1.2×10^{-2}
Mollicutes	Mycoplasmatales	Mycoplasmataceae	Mycoplasma	hyosynoviae	1.5×10^{-3}	3.4×10^{-3}	2.15	1.2×10^{-2}
Genus level								
Bacteroidia	Bacteroidales	Bacteroidaceae	Bacteroides		3.5×10^{-4}	7.4×10^{-5}	2.24	2.1×10^{-3}
Clostridia	Clostridiales	Eubacteriaceae	Eubacterium		7.5×10^{-4}	9.8×10^{-5}	2.92	1.8×10^{-3}
Betaproteobacteria	Burkholderiales	Burkholderiaceae	Lautropia		1.0×10^{-3}	4.1×10^{-3}	−1.99	9.7×10^{-3}
Betaproteobacteria	Neisseriales	Neisseriaceae	Neisseria		1.8×10^{-2}	4.0×10^{-2}	−1.16	9.7×10^{-3}
Spirochaetes	Spirochaetales	Spirochaetaceae	Treponema		1.8×10^{-2}	7.6×10^{-3}	1.27	2.3×10^{-3}
Synergistia	Synergistales	Dethiosulfovibrionaceae	TG5		1.7×10^{-3}	6.0×10^{-4}	1.53	2.3×10^{-3}
Mollicutes	Mycoplasmatales	Mycoplasmataceae	Mycoplasma		1.9×10^{-3}	3.9×10^{-4}	2.28	1.8×10^{-3}
Class level								
Betaproteobacteria					2.2×10^{-2}	5.0×10^{-2}	−0.35	3.9×10^{-2}
Spirochaetes					1.8×10^{-2}	7.6×10^{-3}	0.38	1×10^{-2}
Synergistia					1.7×10^{-3}	6.0×10^{-4}	0.46	1×10^{-2}
Mollicutes					3.2×10^{-3}	1.9×10^{-3}	0.23	3×10^{-2}

wise test on taxon and FNC (Fig. S2) showed that *Neisseria* had significant associations with FNC between functional networks *left angular* and *right inferior occipital gyrus* (*IOG)* (FDR = 0.017) and FNC between *PCC/Precuneus* and *right IOG* (FDR = 0.06), while no significant pair-wise taxon-FNC associations were found in *Treponema* or *TG5*.

Genera *Eubacterium* (class *Clostridia*), *Bacteroides* (class *Bacteroidia*) and *Mycoplasma* (class *Mollicutes*) also had significant associations with FNC loading, suggesting higher microbial abundance related to higher FNC loading and thereby lower connectivity strength of top FNCs in this component. In particular, *Eubacterium* showed significant associations with all top FNCs (FDR<0.05). Both *Bacteroides* and *Mycoplasma* were also related to FNC between left angular and right fusiform/lingual (FDR = 0.04 and 2.6×10^{-3}, respectively). No significant interactions were observed.

Lower-level analysis further identified that the abundance of species from genus *Actinomyces* (class *Actinobacteria*) showed significant positive relationship with FNC loading (logFC = 2.35, FDR = 3.6×10^{-2}) and the association was significantly different between groups (P_interact = 1.1×10^{-7}). *Actinomyces* was specifically associated with FNC between *left angular* and *right Fusiform/Lingual* and FNC between *left angular* and *left middle occipital gyrus (MOG)*. Genus *Prevotella* (class *Bacteroidia*) was significantly associated with FNC loading in both groups and associated with all top contributing FNCs (FDR<0.1).

3.5. Functional metabolism pathway prediction

Among the 262 KEGG pathways predicted for microbial function, we identified 23 pathways showing significant difference in abundance between smokers and nonsmokers after correcting for multiple tests by FDR with threshold 0.15, as shown in Fig. 4. The pathways with significantly altered abundance in smokers mainly involved metabolism and genetic information processing. Enriched metabolic pathways included those involved with metabolism (cofactors and vitamins, terpenoids and polyketides, amino acids, nucleotides, and glycans). Depleted pathways had roles in energy and lipid metabolism, membrane transport, and xenobiotics biodegradation (e.g., drug metabolism-cytochrome P450). In addition, genetic information processing pathways (e.g., proteasome, protein export, nucleotide excision repair, DNA repair and recombination proteins, and ubiquitin system) were also significantly enriched in smokers whereas other pathways related to diseases (i.e., immune disease, neurodegenerative disease), nervous system, and circulatory system were also associated. The results from a larger sample size (n = 128) for validation are shown in Fig. S3. It can be seen that most of pathways, especially neurotransmitter pathways (e.g., Tyrosine metabolism, Glutamatergic synapse), are also identified to be significant (FDR<0.05). Further pair-wise examination of the correlations between microbiota and the functional pathways demonstrated that alterations in the abundance of microbiota were highly correlated to these pathways (mean absolute value of correlation 0.19–0.29 in different taxonomic levels), especially for the genera *Lautropia* and *Neisseria* from class Betaproteobacteria as shown in Fig. S4. The associations between each pathway and rsfMRI FNC loading showed several neurotransmitter pathways marginally associated with FNC loading as shown in Fig. S5, including: D-Glutamine and D-glutamate metabolism (P = 0.07), Tyrosine metabolism (P = 0.03) and Glutamatergic synapse (P = 0.07).

4. Discussion and conclusions

In this work, we set out to determine if there was correlation between shifts in the oral microbiome and changes in brain signaling networks due to smoking. To achieve this, we used 16S rRNA sequencing to characterize the microbial composition in the saliva of participants (smokers versus nonsmokers), and rsfMRI to measure brain functional activity in these same participants. Consistent with previous findings, shifts in the oral microbiome and changes in brain functional activity occurred in smokers. Some oral microbial populations were found to have significant correlation with particular neurological signaling networks. While the influence of the gastrointestinal microbiome on neurological activity has been an area of intense study, this study suggests that the potential role of oral microbiome in relation to neurological signaling, suggesting a new direction for studying the pathology of neurological disorders.

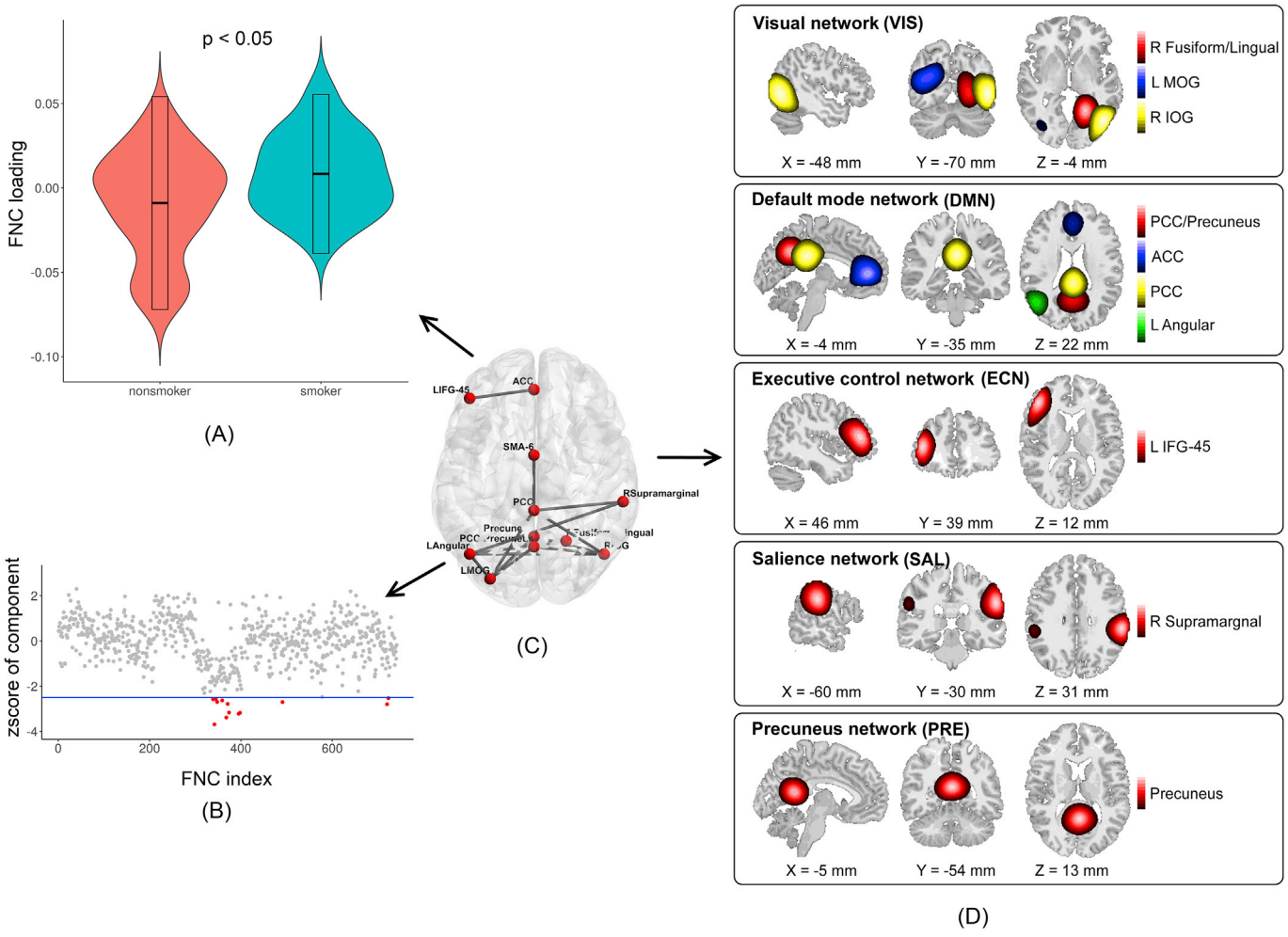

Fig. 3. The loading and spatial mapping of identified FNC component. (A) The loading of identified FNC component in smokers compared to nonsmokers; (B) Top FNCs with z-scored weights absolute (z-score)> 2.5 in the component; (C) The top contributing connectivity among the functional networks from the selected component; (D) Brain regions of those functional networks involved the top FNCs.

Table 3
The associations between smoking-related taxa and FNC component.

Taxa					Association with FNC component				
Class	Order	Family	Genus	Species	Beta	P	FDR	Beta_interact	P_interact
Species level									
Actinobacteria	Actinomycetales	Actinomycetaceae	Actinomyces	spp	29.1	9×10^{-3}	3.6×10^{-2}	−83.2	1.1 × 10-7
Bacteroidia	Bacteroidales	Prevotellaceae	Prevotella	oris	43.2	3.3×10^{-6}	3.9×10^{-5}	−8.4	0.36
Clostridia	Clostridiales	Eubacteriaceae	Eubacterium	saphenum	34.0	4.3×10^{-5}	2.6×10^{-4}	14.4	0.08
Genus level									
Bacteroidia	Bacteroidales	Bacteroidaceae	Bacteroides		15.12	6.6×10^{-2}	7.7×10^{-2}	10.2	0.22
Clostridia	Clostridiales	Eubacteriaceae	Eubacterium		35.09	2.6×10^{-5}	1.9×10^{-4}	11.8	0.14
Betaproteobacteria	Neisseriales	Neisseriaceae	Neisseria		−20.18	4×10^{-2}	7.4×10^{-2}	−28.7	4.8×10^{-3}
Spirochaetes	Spirochaetales	Spirochaetaceae	Treponema		18.78	3.4×10^{-2}	7.4×10^{-2}	19.5	0.044
Synergistia	Synergistales	Dethiosulfovibrionaceae	TG5		13.04	4.2 × 10-2	7.4×10^{-2}	12.4	0.065
Mollicutes	Mycoplasmatales	Mycoplasmataceae	Mycoplasma		13.13	6.5×10^{-2}	7.7×10^{-2}	11.5	0.11
Class level									
Betaproteobacteria					−20.15	3.9 × 10-2	5 × 10-2	−24.3	1.7×10^{-2}
Synergistia					14.80	3×10^{-2}	5×10^{-2}	12.7	7.7×10^{-2}
Mollicutes					18.76	1.7×10^{-2}	5×10^{-2}	16.3	3.9×10^{-2}

Results from 16S rRNA sequencing demonstrated significant changes in microbial composition by both unweighted UniFrac and Bray-Curtis distances between smokers than nonsmokers, suggesting less microbial diversity in the salivary microbiome of smokers. Furthermore, shifts in taxonomic abundance by smoking were consistent with previous studies. For instances, gram-negative bacteria from the genera *Lautropia* and *Neisseria* (class *Betaproteobacteria*) showed depletion in the smokers, in line with previous reports (Kumar et al., 2011; Shchipkova et al., 2010). Several in vitro studies have also demonstrated a strong inhibitory effect on smoking in *Neisseria* growth (Bardell, 1981). On the other hand, smoking led to an opposite effect on a number of taxa including the enrichment of *Bacteroides* (Valles et al., 2018), *Treponema* (Kumar et al.,

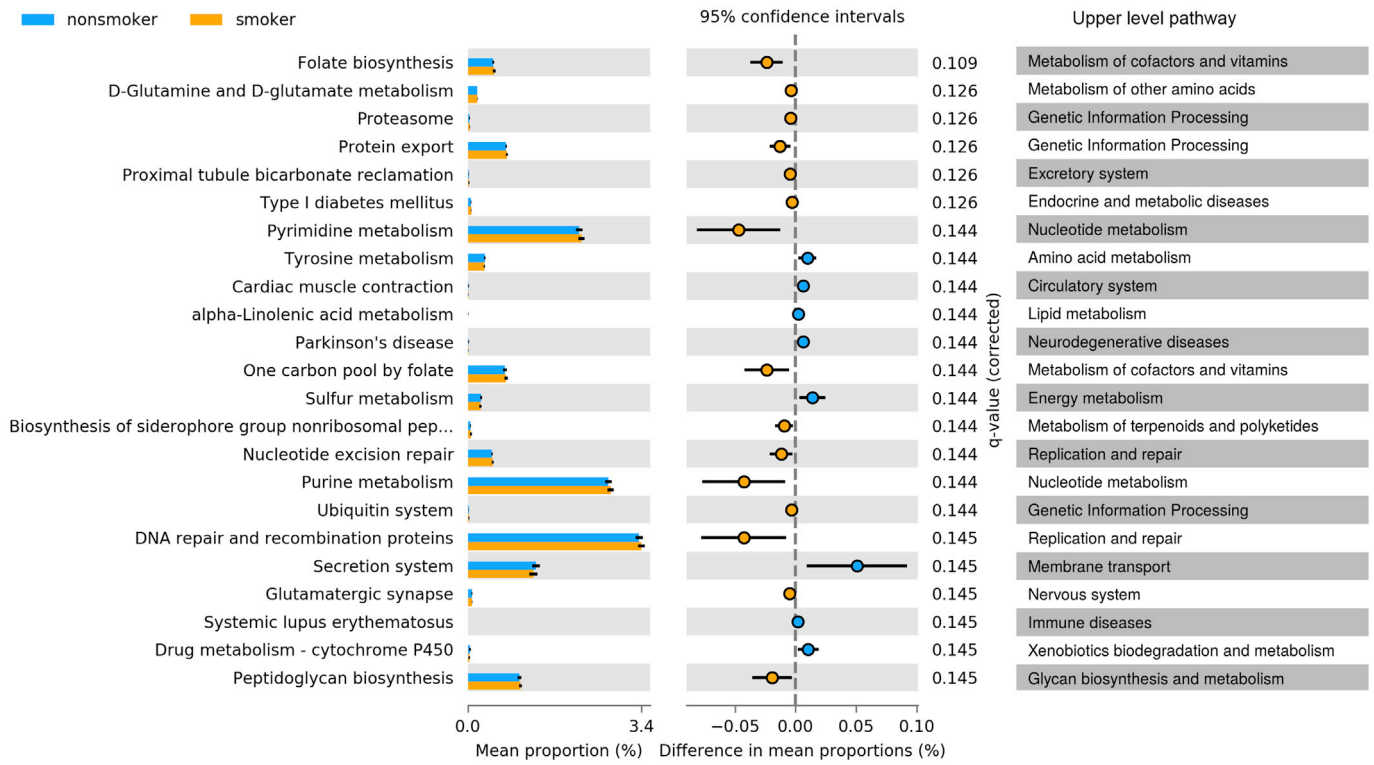

Fig. 4. Pathway enrichment analysis based on the predicted metagenomics. The 23 out of 262 KEGG functional pathways show significant changes in abundance between smokers and nonsmokers (FDR < 0.15). Those pathways were predicted from 16S rRNA microbiome sequencing using the PICRUSt algorithm. Mean proportion (colored bar) indicates the relative abundance of the pathway in each group. The difference of mean proportions between groups as well as the 95% confidence interval indicates the effect size of relative abundance change for each pathway.

2011), *TG5* and *Mycoplasma* (Valles et al., 2018). This enrichment may be indicative of increased inflammation within the oral cavity, especially *Mycoplasma* is thought to synergize with smoking to produce the pro-inflammatory environment (Martin et al., 2006). In addition, low-level analysis identified some species significantly enriched in smokers. *Actinomyces* spp. from the gram-negative class *Actinobacteria* shows increased abundance in smokers, in line with previous large scale oral microbiome study (Wu et al., 2016). *Tannerella forsythia* has been reported to enrich in subgingival plaque of current smokers and demonstrated potential risk as pathogen to induce periodontal disease (Guglielmetti et al., 2014). *Prevotella oris* and *Prevotella* spp. from *Bacteroidales* are coaggregated with Porphyromonas gingivalis (Sato and Nakazawa, 2014) which is also a critical periodontitis pathogen and is highly promoted during the infection by smoking (Zeller et al., 2014). Most of these enriched microbiota are anaerobes compared to aerobic *Neisseria*, consistent with the finding of higher abundance of anaerobes in subgingival plaque samples of smokers, suggesting the depleting of oxygen in oral cavity induced by smoking (Mason et al., 2015).

KEGG pathway analysis identified several metabolic pathways involved in functional changes during smoking. This is perhaps not surprising as cigarette smoke has been reported to be highly associated with DNA damage, lipid peroxidation and antioxidant impairment, and protein modification and misfolding, thereby inducing severe cellular damage (van Rijt et al., 2012; Solak et al., 2005). These influences may affect the oral microbiome community with its direct proximity to toxins from cigarette smoking. We found significant enrichment of metabolic pathways involving the proteasome, protein export and the ubiquitin system. All of them are related to protein degradation and recycling in the cell, which is essential for cellular processes such as proliferation, signaling, and immune responses (Bader and Steller, 2009). The up-regulation of these pathways indicates the role of smoking in disrupting protein modification and cellular processes of the microbial constituents within the oral cavity. Other pathways related to DNA repair and replication-including folate biosynthesis-were also significantly activated in the oral microbiome of smokers. The involvement of proteasome function and DNA repair pathways enhanced in the smoking population may be due to increased cellular dysfunction and DNA damage induced by smoking. Additionally, enrichment was also found in pathways related to small amino acid production such as glutamate and glutamine, glutamatergic synapse and tyrosine metabolism, which are related to neurotransmitter release and potentially interact with nervous system in changing neuronal activity of smokers such as addiction and craving (Fernstrom and Fernstrom, 2007; Dani et al., 2001). On the contrary, some metabolisms are significantly depleted in smokers such as metabolisms of lipid energy (i.e., alpha-linolenic and sulfur), and xenobiotics biodegradation (i.e., drug metabolism-cytochrome P450), which is in line with previous studies (Wu et al., 2016; Rise et al., 2009).

Neuroimaging analysis identified one smoking-related FNC component mainly involved in the connectivity between DMN and other task-positive networks from VIS, SAL, ECN and PRE domains, which is overlapped with the report in our previous study (Vergara et al., 2017). Several novel functional networks were identified in this study which may due to the difference in the analysis method. Instead of testing each FNC individually, we applied a multivariate method (i.e., ICA) to account for the covariance structure among FNCs and clustered those FNCs into one component. We can see that most of these 13 FNCs link DMN and other task-positive networks, suggesting their correlated patterns across individuals. Although these FNCs may present weak effect individually in previous work, their combined effect is expected to be detected by multivariate method as demonstrated in other multivariate analysis studies (Liu and Calhoun, 2014; Lin et al., 2014).

Among the top functional networks in identified smoking-related FNC component, DMN is mostly related to self-referential and episodic memory processing, which is down-regulated in task performance (Gusnard et al., 2001). The other networks are activated corresponding to different tasks such as visual, cognitive control, attention and

moment-to-moment information processing, namely 'task-positive' regions (Fox et al., 2005). Functional MRI studies in both task performance and resting state have reported tight coupling between DMN and other task positive networks with negative correlations (anti-correlation) (Fox et al., 2005, 2006; Uddin et al., 2009). In our work, we found similar anti-correlations between DMN and the other domains (e.g., VIS, SAL and ECN) with reduced connectivity (i.e., increased negative coupling) in smokers when compared to nonsmokers. Reduced connectivity within and between DMN and ECN networks were also reported in chronic smokers compared to nonsmokers, showing larger decreases of connectivity with heavier nicotine use (Weiland et al., 2015). Additional studies found increased coupling among medial orbital prefrontal cortex, the dorsal medial PFC, striatum, and visual cortex over the course of 1 h acute abstinence, suggesting the change of connectivity among DMN domain, rewarding circuit and VIS in relation to cigarette craving (Janes et al., 2014). Our results combined with the above findings suggest dynamic modulation in functional coupling between DMN and task-positive networks when subjects smoke or go through withdrawal as compared to nonsmokers.

By correlating changes in oral microbial abundance with the smoking-related brain FNC component, we identified several microbiota related to brain function although they were not changed by smoking. *Prevotella oris* (class *Bacteroidia*), a common gram-negative, anaerobic bacterium of the normal oral flora has been shown to significantly associate with most of top contributing FNCs in the FNC component. It is related to the development of brain abscess and other neurological syndromes (i.e., Lemierre's syndrome) through production of IgA proteases to promote virulence and initiate an immune response (Wu et al., 2014; Garza-Alatorre et al., 2015). Another member of the class *Bacteroidia*, *genus Bacteroides*, has the ability to produce complex, pro-inflammatory neurotoxins that may induce inflammation in oral cavity and further contribute to development of inflammation in the brain, increasing brain-blood-barrier permeability through the circulatory system (Lukiw, 2016). Similarly, genus *Mycoplasma* has been reported to interact with smoking to produce a destructive type of inflammatory response in causing respiratory disease (Kariya et al., 2008). All of these bacteria are associated with one or more top FNCs in the component. In particular, the FNC between functional network *left angular* gyrus and *fusiform/lingual* gyrus is related to all of bacteria. Left angular gyrus is a brain region from DMN connectivity involving information processing, recognition and attention, which will be deactivated during effortful tasks (Seghier et al., 2010) while fusiform/lingual gyrus is mainly related to visual or language information processing and will be activated during tasks. The anti-correlation between both functional networks is significantly associated with those pro-inflammatory bacteria, suggesting the contribution of inflammatory pathway in mediating the influence of microbiome in neurological processes on information processing.

Some microbiota were associated with brain connectivity but the associations can be changed by smoking. Genus *Neisseria* is negatively associated with FNC loading, especially the FNC between network left angular gyrus and right inferior occipital gyrus (FDR = 0.017) related to visual processing function. The genus, including species *Neisseria meningitidis*, stimulates the immune system through a variety of mechanisms (e.g., the production of lipopolysaccharide endotoxin) and invades the neurological nervous system during infection (Pizza and Rappuoli, 2015). Species *Actinomyces* spp., anaerobic Gram-positive bacteria, is also significantly associated with FNC component, mainly including FNCs between left angular gyrus and fusiform/lingual gyrus and middle occipital gyrus, which are related to visual recognition and processing. *Actinomyces* spp. has been reported to cause a rare chronic disease-'*Actinomycosis*' with typical clinic presentation such as pulmonary actinomycosis in smokers with poor dental hygiene (Valour et al., 2014). Similarly, *Treponema* infects the brain via branches of the trigeminal nerve (Riviere et al., 2002). In this study, we demonstrate that these bacteria have significant associations with brain function alternated by smoking, suggesting potential pathways (i.e., inflammatory pathways) for smoking to influence the relationship between oral microbiome and neurological activity (i.e., recognition and visual processing) in the brain, similar to how gut microbiome-brain interactions occur (Carabotti et al., 2015).

Along the gut-brain axis, neurotransmitter signaling pathways play important roles in bidirectional modulation of brain function. Our functional pathway prediction analysis identified enrichment in several neurotransmitter-related pathways among oral microbiota such as glutamate-glutamine, tyrosine metabolism, and glutamatergic synapse. Production of neurotransmitters from these pathways (i.e., glutamate and glutamine) is stimulated by smoking and they are highly involved in reward circuit neural functions for smoking dependence (Benowitz, 2010; De Biasi and Dani, 2011) and the interactions between DMN and other task-related networks (Hu et al., 2013). These neurotransmitter pathways are marginally associated with identified FNC loading and also show high correlations with some FNC-related microbiota, suggesting the potential of these specific microbiota together with other oral microbiota to influence brain function through neurotransmitter signaling pathways.

This study explores the association between fluctuations within the oral microbiome and the brain functional network in smokers. While these associations suggest underlying biological pathways for microbiome-brain link, we are unable to assess a causal relationship among the features. Some interesting but marginal signals were shown in pathway analysis with a more lenient FDR <0.15 cut-off due to the limit sample size in each group. Although the results from a larger sample size show the improvement in statistical significance on most pathways, more systematic validations are desired. Additionally, although we tried to control for alcohol consumption and marijuana smoking score, their complex interactions with cigarette smoking with respect to the oral microbiome community and brain function may still confound our results. As such, follow on studies should employ stricter criteria for selection of the smoking and non-smoking control group are suggested. Despite these limitations, this study represents the first evidence of correlation between population shifts within the oral microbiome and changes in neurological signaling. As the oral cavity is an easily accessible environment, as compared to the gastrointestinal tract, further study offers opportunity for development of novel therapeutics for neurological syndromes.

Competing interests

The authors declare that they have no competing interests.

Acknowledgements

This work was supported by the National Institutes of Health [grant numbers P20GM103472, R01EB005846, and K23AA026635], and National Science Foundation, grant number: 1539067.

Appendix A. Supplementary data

Supplementary data to this article can be found online at https://doi.org/10.1016/j.neuroimage.2019.06.023.

References

Astafurov, K., Elhawy, E., Ren, L., Dong, C.Q., Igboin, C., Hyman, L., Griffen, A., Mittag, T., Danias, J., 2014. Oral microbiome link to neurodegeneration in glaucoma. PLoS One 9 (9), e104416.

Babor, T.F., Higgins-Biddle, J.C., Saunders, J.B., Monteiro, M.G., Organization, W.H., 2001. AUDIT: the Alcohol Use Disorders Identification Test: Guidelines for Use in Primary Health Care.

Bader, M., Steller, H., 2009. Regulation of cell death by the ubiquitin–proteasome system. Curr. Opin. Cell Biol. 21 (6), 878–884.

Bagga, D., Aigner, C.S., Reichert, J.L., Cecchetto, C., Fischmeister, F.P.S., Holzer, P., Moissl-Eichinger, C., Schöpf, V., 2018. Influence of 4-week multi-strain probiotic administration on resting-state functional connectivity in healthy volunteers. Eur. J. Nutr. 1–7.

Bardell, D., 1981. Viability of six species of normal oropharyngeal bacteria after exposure to cigarette smoke in vitro. Microbios 32 (127), 7–13.
Benowitz, N.L., 2010. Nicotine addiction. N. Engl. J. Med. 362 (24), 2295–2303.
Borre, Y.E., O'Keeffe, G.W., Clarke, G., Stanton, C., Dinan, T.G., Cryan, J.F., 2014. Microbiota and neurodevelopmental windows: implications for brain disorders. Trends Mol. Med. 20 (9), 509–518.
Calhoun, V.D., Adali, T., Pearlson, G.D., Pekar, J., 2001. A method for making group inferences from functional MRI data using independent component analysis. Hum. Brain Mapp. 14 (3), 140–151.
Callahan, B.J., McMurdie, P.J., Rosen, M.J., Han, A.W., Johnson, A.J.A., Holmes, S.P., 2016. DADA2: high-resolution sample inference from Illumina amplicon data. Nat. Methods 13 (7), 581.
Camelo-Castillo, A.J., Mira, A., Pico, A., Nibali, L., Henderson, B., Donos, N., Tomas, I., 2015. Subgingival microbiota in health compared to periodontitis and the influence of smoking. Front. Microbiol. 6, 119.
Cao, X., 2017. Intestinal inflammation induced by oral bacteria. Science 358 (6361), 308–309.
Carabotti, M., Scirocco, A., Maselli, M.A., Severi, C., 2015. The gut-brain axis: interactions between enteric microbiota, central and enteric nervous systems. Ann. Gastroenterol. Q. Publ. Hell. Soc. Gastroenterol. 28 (2), 203.
Chen, T., Yu, W.-H., Izard, J., Baranova, O.V., Lakshmanan, A., Dewhirst, F.E., 2010. The Human Oral Microbiome Database: a web accessible resource for investigating oral microbe taxonomic and genomic information. Database 2010.
Cole, D.M., Beckmann, C.F., Long, C.J., Matthews, P.M., Durcan, M.J., Beaver, J.D., 2010. Nicotine replacement in abstinent smokers improves cognitive withdrawal symptoms with modulation of resting brain network dynamics. Neuroimage 52 (2), 590–599.
Collins, S.M., Surette, M., Bercik, P., 2012. The interplay between the intestinal microbiota and the brain. Nat. Rev. Microbiol. 10 (11), 735.
Dani, J.A., Ji, D., Zhou, F.M., 2001. Synaptic plasticity and nicotine addiction. Neuron 31 (3), 349–352.
De Biasi, M., Dani, J.A., 2011. Reward, addiction, withdrawal to nicotine. Annu. Rev. Neurosci. 34, 105–130.
Dewhirst, F.E., Chen, T., Izard, J., Paster, B.J., Tanner, A.C., Yu, W.-H., Lakshmanan, A., Wade, W.G., 2010. The human oral microbiome. J. Bacteriol. 192 (19), 5002–5017.
Erhardt, E.B., Rachakonda, S., Bedrick, E.J., Allen, E.A., Adali, T., Calhoun, V.D., 2011. Comparison of multi-subject ICA methods for analysis of fMRI data. Hum. Brain Mapp. 32 (12), 2075–2095.
Fedota, J.R., Stein, E.A., 2015. Resting-state functional connectivity and nicotine addiction: prospects for biomarker development. Ann. N. Y. Acad. Sci. 1349, 64–82.
Fernstrom, J.D., Fernstrom, M.H., 2007. Tyrosine, phenylalanine, and catecholamine synthesis and function in the brain. J. Nutr. 137 (6 Suppl. 1), 1539S–1547S discussion 1548S.
Foster, J.A., Neufeld, K.-A.M., 2013. Gut–brain axis: how the microbiome influences anxiety and depression. Trends Neurosci. 36 (5), 305–312.
Fox, M.D., Snyder, A.Z., Vincent, J.L., Corbetta, M., Van Essen, D.C., Raichle, M.E., 2005. The human brain is intrinsically organized into dynamic, anticorrelated functional networks. Proc. Natl. Acad. Sci. U. S. A. 102 (27), 9673–9678.
Fox, M.D., Corbetta, M., Snyder, A.Z., Vincent, J.L., Raichle, M.E., 2006. Spontaneous neuronal activity distinguishes human dorsal and ventral attention systems. Proc. Natl. Acad. Sci. Unit. States Am. 103 (26), 10046–10051.
Gareau, M.G., Wine, E., Rodrigues, D.M., Cho, J.H., Whary, M.T., Philpott, D.J., MacQueen, G., Sherman, P.M., 2011. Bacterial infection causes stress-induced memory dysfunction in mice. Gut 60 (3), 307–317.
Garza-Alatorre, A., Hernández-Rosales, C., Rodríguez-Coronado, J., Solís-González, M.C., Balderrama-Dávila, R., Rosiles-De la Garza, S.G., 2015. Atypical Lemierre's syndrome caused by Prevotella oris. Med. Univ. 17 (69), 218–221.
Guglielmetti, M.R., Rosa, E.F., Lourencao, D.S., Inoue, G., Gomes, E.F., De Micheli, G., Mendes, F.M., Hirata, R.D., Hirata, M.H., Pannuti, C.M., 2014. Detection and quantification of periodontal pathogens in smokers and never-smokers with chronic periodontitis by real-time polymerase chain reaction. J. Periodontol. 85 (10), 1450–1457.
Gusnard, D.A., Akbudak, E., Shulman, G.L., Raichle, M.E., 2001. Medial prefrontal cortex and self-referential mental activity: relation to a default mode of brain function. Proc. Natl. Acad. Sci. U. S. A. 98 (7), 4259–4264.
Heatherton, T.F., Kozlowski, L.T., Frecker, R.C., Fagerstrom, K.O., 1991. The Fagerstrom test for nicotine dependence: a revision of the Fagerstrom tolerance Questionnaire. Br. J. Addict. 86 (9), 1119–1127.
Hong, L.E., Gu, H., Yang, Y., Ross, T.J., Salmeron, B.J., Buchholz, B., Thaker, G.K., Stein, E.A., 2009. Association of nicotine addiction and nicotine's actions with separate cingulate cortex functional circuits. Arch. Gen. Psychiatr. 66 (4), 431–441.
Hu, Y., Chen, X., Gu, H., Yang, Y., 2013. Resting-state glutamate and GABA concentrations predict task-induced deactivation in the default mode network. J. Neurosci. Off. J. Soc. Neurosci. 33 (47), 18566–18573.
Janes, A.C., Pizzagalli, D.A., Richardt, S., de, B.F.B., Chuzi, S., Pachas, G., Culhane, M.A., Holmes, A.J., Fava, M., Evins, A.E., et al., 2010. Brain reactivity to smoking cues prior to smoking cessation predicts ability to maintain tobacco abstinence. Biol. Psychiatry 67 (8), 722–729.
Janes, A.C., Farmer, S., Nickerson, L.D., Lukas, S.E., 2014. An increase in tobacco craving is associated with enhanced medial prefrontal cortex network coupling. PLoS One 9 (2), e88228.
Jiang, H., Ling, Z., Zhang, Y., Mao, H., Ma, Z., Yin, Y., Wang, W., Tang, W., Tan, Z., Shi, J., et al., 2015. Altered fecal microbiota composition in patients with major depressive disorder. Brain Behav. Immun. 48, 186–194.
Kanehisa, M., Goto, S., 2000. KEGG: kyoto encyclopedia of genes and genomes. Nucleic Acids Res. 28 (1), 27–30.
Kariya, C., Chu, H.W., Huang, J., Leitner, H., Martin, R.J., Day, B.J., 2008. Mycoplasma pneumoniae infection and environmental tobacco smoke inhibit lung glutathione adaptive responses and increase oxidative stress. Infect. Immun. 76 (10), 4455–4462.
Katoh, K., Standley, D.M., 2013. MAFFT multiple sequence alignment software version 7: improvements in performance and usability. Mol. Biol. Evol. 30 (4), 772–780.
Kumar, P.S., Matthews, C.R., Joshi, V., de Jager, M., Aspiras, M., 2011. Tobacco smoking affects bacterial acquisition and colonization in oral biofilms. Infect. Immun. 79 (11), 4730–4738.
Langille, M.G., Zaneveld, J., Caporaso, J.G., McDonald, D., Knights, D., Reyes, J.A., Clemente, J.C., Burkepile, D.E., Thurber, R.L.V., Knight, R., 2013. Predictive functional profiling of microbial communities using 16S rRNA marker gene sequences. Nat. Biotechnol. 31 (9), 814.
Lin, D., Calhoun, V.D., Wang, Y.-P., 2014. Correspondence between fMRI and SNP data by group sparse canonical correlation analysis. Med. Image Anal. 18 (6), 891–902.
Liu, J., Calhoun, V.D., 2014. A review of multivariate analyses in imaging genetics. Front. Neuroinf. 8, 29.
Lukiw, W.J., 2016. Bacteroides fragilis lipopolysaccharide and inflammatory signaling in Alzheimer's disease. Front. Microbiol. 7, 1544.
Ma, S., Correa, N.M., Li, X.-L., Eichele, T., Calhoun, V.D., Adali, T., 2011. Automatic identification of functional clusters in FMRI data using spatial dependence. IEEE (Inst. Electr. Electron. Eng.) Trans. Biomed. Eng. 58 (12), 3406–3417.
Macgregor, I., 1989. Effects of smoking on oral ecology. A review of the literature. Clin. Prev. Dent. 11 (1), 3–7.
Martin, R.J., Wexler, R.B., Day, B.J., Harbeck, R.J., Pinkerton, K.E., Chu, H.W., 2006. Interaction between cigarette smoke and mycoplasma infection: a murine model. COPD 3 (1), 3–8.
Mason, M.R., Preshaw, P.M., Nagaraja, H.N., Dabdoub, S.M., Rahman, A., Kumar, P.S., 2015. The subgingival microbiome of clinically healthy current and never smokers. ISME J. 9 (1), 268–272.
Moran, L.V., Sampath, H., Stein, E.A., Hong, L.E., 2012. Insular and anterior cingulate circuits in smokers with schizophrenia. Schizophr. Res. 142 (1–3), 223–229.
Morris, A., Beck, J.M., Schloss, P.D., Campbell, T.B., Crothers, K., Curtis, J.L., Flores, S.C., Fontenot, A.P., Ghedin, E., Huang, L., 2013. Comparison of the respiratory microbiome in healthy nonsmokers and smokers. Am. J. Respir. Crit. Care Med. 187 (10), 1067–1075.
Mulle, J.G., Sharp, W.G., Cubells, J.F., 2013. The gut microbiome: a new frontier in autism research. Curr. Psychiatr. Rep. 15 (2), 337.
Oksanen, J., Kindt, R., Legendre, P., O'Hara, B., Stevens, M.H.H., Oksanen, M.J., Suggests, M., 2007. The vegan package. Commun. Ecol. Package 10, 631–637.
O'mahony, S., Clarke, G., Borre, Y., Dinan, T., Cryan, J., 2015. Serotonin, tryptophan metabolism and the brain-gut-microbiome axis. Behav. Brain Res. 277, 32–48.
Parks, D.H., Tyson, G.W., Hugenholtz, P., Beiko, R.G., 2014. STAMP: statistical analysis of taxonomic and functional profiles. Bioinformatics 30 (21), 3123–3124.
Paulson, J.N., Stine, O.C., Bravo, H.C., Pop, M., 2013. Differential abundance analysis for microbial marker-gene surveys. Nat. Methods 10 (12), 1200.
Pereira, P.A., Aho, V.T., Paulin, L., Pekkonen, E., Auvinen, P., Scheperjans, F., 2017. Oral and nasal microbiota in Parkinson's disease. Park. Relat. Disord. 38, 61–67.
Pinto-Sanchez, M.I., Hall, G.B., Ghajar, K., Nardelli, A., Bolino, C., Lau, J.T., Martin, F.-P., Cominetti, O., Welsh, C., Rieder, A., 2017. Probiotic Bifidobacterium longum NCC3001 reduces depression scores and alters brain activity: a pilot study in patients with irritable bowel syndrome. Gastroenterology 153 (2), 448–459 e448.
Pizza, M., Rappuoli, R., 2015. Neisseria meningitidis: pathogenesis and immunity. Curr. Opin. Microbiol. 23, 68–72.
Power, J.D., Barnes, K.A., Snyder, A.Z., Schlaggar, B.L., Petersen, S.E., 2012. Spurious but systematic correlations in functional connectivity MRI networks arise from subject motion. Neuroimage 59 (3), 2142–2154.
Quigley, E.M.M., 2017. Microbiota-brain-gut Axis and neurodegenerative diseases. Curr. Neurol. Neurosci. Rep. 17 (12), 94.
Rideout, J.R., He, Y., Navas-Molina, J.A., Walters, W.A., Ursell, L.K., Gibbons, S.M., Chase, J., McDonald, D., Gonzalez, A., Robbins-Pianka, A., et al., 2014. Subsampled open-reference clustering creates consistent, comprehensive OTU definitions and scales to billions of sequences. PeerJ 2, e545.
Rise, P., Ghezzi, S., Manzoni, C., Colombo, C., Galli, C., 2009. The in vitro effects of cigarette smoke on fatty acid metabolism are partially counteracted by simvastatin. Prostagl. Leukot. Essent. Fat. Acids 80 (1), 71–75.
Riviere, G.R., Riviere, K., Smith, K., 2002. Molecular and immunological evidence of oral Treponema in the human brain and their association with Alzheimer's disease. Oral Microbiol. Immunol. 17 (2), 113–118.
Round, J.L., Lee, S.M., Li, J., Tran, G., Jabri, B., Chatila, T.A., Mazmanian, S.K., 2011. The Toll-like receptor 2 pathway establishes colonization by a commensal of the human microbiota. Science 1206095.
Said, H.S., Suda, W., Nakagome, S., Chinen, H., Oshima, K., Kim, S., Kimura, R., Iraha, A., Ishida, H., Fujita, J., et al., 2014. Dysbiosis of salivary microbiota in inflammatory bowel disease and its association with oral immunological biomarkers. DNA Res. Int. J. Rapid Publ. Rep. Genes Genomes 21 (1), 15–25.
Sato, T., Nakazawa, F., 2014. Coaggregation between Prevotella oris and Porphyromonas gingivalis. J. Microbiol. Immunol. Infect. 47 (3), 182–186.
Seghier, M.L., Fagan, E., Price, C.J., 2010. Functional subdivisions in the left angular gyrus where the semantic system meets and diverges from the default network. J. Neurosci. : Off. J. Soc. Neurosci. 30 (50), 16809–16817.
Shchipkova, A.Y., Nagaraja, H.N., Kumar, P.S., 2010. Subgingival microbial profiles of smokers with periodontitis. J. Dent. Res. 89 (11), 1247–1253.
Shoemark, D.K., Allen, S.J., 2015. The microbiome and disease: reviewing the links between the oral microbiome, aging, and Alzheimer's disease. J. Alzheimer's Dis. 43 (3), 725–738.

Solak, Z.A., Kabaroglu, C., Cok, G., Parildar, Z., Bayindir, U., Ozmen, D., Bayindir, O., 2005. Effect of different levels of cigarette smoking on lipid peroxidation, glutathione enzymes and paraoxonase 1 activity in healthy people. Clin. Exp. Med. 5 (3), 99–105.
Spear, L.P., 2018. Effects of adolescent alcohol consumption on the brain and behaviour. Nat. Rev. Neurosci. 19 (4), 197.
Sudo, N., Chida, Y., Aiba, Y., Sonoda, J., Oyama, N., Yu, X.N., Kubo, C., Koga, Y., 2004. Postnatal microbial colonization programs the hypothalamic–pituitary–adrenal system for stress response in mice. J. Physiol. 558 (1), 263–275.
Tanabe, J., Nyberg, E., Martin, L.F., Martin, J., Cordes, D., Kronberg, E., Tregellas, J.R., 2011. Nicotine effects on default mode network during resting state. Psychopharmacology 216 (2), 287–295.
Tillisch, K., Labus, J., Kilpatrick, L., Jiang, Z., Stains, J., Ebrat, B., Guyonnet, D., Legrain-Raspaud, S., Trotin, B., Naliboff, B., et al., 2013. Consumption of fermented milk product with probiotic modulates brain activity. Gastroenterology 144 (7), 1394–1401, 1401 e1391-1394.
Uddin, L.Q., Kelly, A.M., Biswal, B.B., Castellanos, F.X., Milham, M.P., 2009. Functional connectivity of default mode network components: correlation, anticorrelation, and causality. Hum. Brain Mapp. 30 (2), 625–637.
Valles, Y., Inman, C.K., Peters, B.A., Ali, R., Wareth, L.A., Abdulle, A., Alsafar, H., Anouti, F.A., Dhaheri, A.A., Galani, D., et al., 2018. Types of tobacco consumption and the oral microbiome in the United Arab Emirates healthy future (UAEHFS) pilot study. Sci. Rep. 8 (1), 11327.
Valour, F., Senechal, A., Dupieux, C., Karsenty, J., Lustig, S., Breton, P., Gleizal, A., Boussel, L., Laurent, F., Braun, E., et al., 2014. Actinomycosis: etiology, clinical features, diagnosis, treatment, and management. Infect. Drug Resist. 7, 183–197.
van Rijt, S.H., Keller, I.E., John, G., Kohse, K., Yildirim, A.O., Eickelberg, O., Meiners, S., 2012. Acute cigarette smoke exposure impairs proteasome function in the lung. Am. J. Physiol. Lung Cell Mol. Physiol. 303 (9), L814–L823.
Vergara, V.M., Liu, J., Claus, E.D., Hutchison, K., Calhoun, V., 2017. Alterations of resting state functional network connectivity in the brain of nicotine and alcohol users. Neuroimage 151, 45–54.
Wade, W.G., 2013. The oral microbiome in health and disease. Pharmacol. Res. 69 (1), 137–143.
Warinner, C., Rodrigues, J.F., Vyas, R., Trachsel, C., Shved, N., Grossmann, J., Radini, A., Hancock, Y., Tito, R.Y., Fiddyment, S., et al., 2014. Pathogens and host immunity in the ancient human oral cavity. Nat. Genet. 46 (4), 336–344.
Weiland, B.J., Sabbineni, A., Calhoun, V.D., Welsh, R.C., Hutchison, K.E., 2015. Reduced executive and default network functional connectivity in cigarette smokers. Hum. Brain Mapp. 36 (3), 872–882.
Wu, P.-C., Tu, M.-S., Lin, P.-H., Chen, Y.-S., Tsai, H.-C., 2014. Prevotella brain abscesses and stroke following dental extraction in a young patient: a case report and review of the literature. Intern. Med. 53 (16), 1881–1887.
Wu, J., Peters, B.A., Dominianni, C., Zhang, Y., Pei, Z., Yang, L., Ma, Y., Purdue, M.P., Jacobs, E.J., Gapstur, S.M., et al., 2016. Cigarette smoking and the oral microbiome in a large study of American adults. ISME J. 10 (10), 2435–2446.
Zeller, I., Hutcherson, J.A., Lamont, R.J., Demuth, D.R., Gumus, P., Nizam, N., Buduneli, N., Scott, D.A., 2014. Altered antigenic profiling and infectivity of Porphyromonas gingivalis in smokers and non-smokers with periodontitis. J. Periodontol. 85 (6), 837–844.